

Direct Fuzzy Adaptive Control for Standalone Wind Energy Conversion Systems

Hoa M. Nguyen, *Member, IAENG* and D. S. Naidu.

Abstract—This paper presents a direct fuzzy adaptive control for standalone Wind Energy Conversion Systems (WECS) with Permanent Magnet Synchronous Generators (PMSG). The problem of maximizing power conversion from intermittent wind of time-varying, highly nonlinear WECS is dealt with by an adaptive control algorithm. The adaptation is designed based on the *Lyapunov* theory and carried out by the fuzzy logic technique. Comparison between the proposed method and the feedback linearization method is shown by numerical simulations verifying the effectiveness of the suggested adaptive control scheme.

Index Terms—wind energy conversion system, permanent magnet synchronous generators, fuzzy logic, nonlinear adaptive control.

I. INTRODUCTION

WIND energy is a renewable energy source. It has developed significantly in the last few decades and now has the fastest growth among other renewable energy sources [1].

Wind energy is harvested by WECS or wind turbines. These wind energy converters can be classified as grid-connected or standalone depending on their connections to utility grids or local grids. Nowadays most WECS are connected to utility grids. However there is still demand for standalone WECS which provide electrical power for remote areas where utility grids cannot reach. To guarantee continuous energy supply, standalone WECS are combined with other energy sources such as battery storage systems, solar energy systems, diesel generators, etc. resulting in Hybrid Wind Energy Systems (HWES). Due to the presence of other energy sources, the control of HWES is quite different from that of grid-connected WECS. Beside attempting to capture as much power as possible, controllers need to ensure constant power flow to local loads. A number of control strategies has been proposed for HWES in [2], [3], [4]. Most of these works focus on the interaction between WECS and storage systems. Meanwhile, authors in [5] deal with the control of maximizing the power conversion of WECS in HWES based on the nonlinear feedback linearization control method.

The adaptive control is an attractive control which provides controllers ability to learn as systems and/or environments change [6]. This feature is particularly useful for WECS which are immersed in highly stochastic wind surroundings. Different adaptive structures were presented to WECS in [7]–[12]. Basically these works study adaptive Proportional Integral Derivative (PID) control using fuzzy logic [7], [8]

or neural networks [9]–[12] to tune PID parameters. Our paper focuses on an adaptive control scheme based on the input-output linearization control where the adaptive rule is designed based on the *Lyapunov* analysis. The chosen HWES is the same as in [5]. The results of the adaptive control will be compared to that of the feedback linearization control in [5] proving advantages of the proposed control.

The paper is organized as follows. Section II describes the HWES and the standalone PMSG-based WECS nonlinear model. The adaptive control design is presented in Section III followed by its application to the standalone WECS in Section IV. Based on simulation results shown in Section V, some discussions and conclusions are drawn in Section VI.

II. STANDALONE WIND ENERGY CONVERSION SYSTEM MODELING

A HWES includes a WECS interacting with another source of energy as shown in Fig. 1. Due to the output power from the WECS fluctuating according to wind changes, other energy sources such as battery or solar systems or diesel generators must be added to ensure a constant power supply to the local grid. Maximum power conversion of the WECS is obtained by adjusting the generator speed ω_g as wind speed V changes. This is achieved by modifying the equivalent load at the generator terminal via power electronics converters. The equivalent standalone WECS is depicted in Fig. 2 where R_L and L_L are the equivalent load resistance and inductance, respectively. The equivalent load resistance is considered the control input for the control system.

The dynamic model of the standalone WECS is obtained by combining the aerodynamics, drive train dynamics and generator dynamics. Note that the power electronics dynamics is ignored because it is much faster than the other dynamics.

The aerodynamics converts wind flows into aerodynamic torque and mechanical power given respectively as

$$T_r = \frac{1}{2} \rho \pi R^3 V^2 C_Q(\lambda, \beta), \quad (1)$$

$$P_r = \frac{1}{2} \rho \pi R^2 V^3 C_P(\lambda, \beta), \quad (2)$$

where T_r is the aerodynamic torque, ρ is the air density, R is the radius of the wind rotor swept area, V is the wind speed, $C_Q(\lambda, \beta)$ is the torque coefficient, P_r is the mechanical power, and $C_P(\lambda, \beta)$ is the power coefficient. It is seen that both torque and power coefficient are functions of the so-called tip-speed ratio λ and pitch angle of the wind rotor blades β . The tip-speed ratio is defined as the ratio between the speed at the tip of blades and the wind speed, which is given as

$$\lambda = \frac{\omega_r R}{V}, \quad (3)$$

Manuscript received July 02, 2012; revised July 31, 2012.

Hoa M. Nguyen is with the Department of Electrical Engineering, Idaho State University, Pocatello, ID, 83201 USA e-mail: nguyhoah@isu.edu.

D. S. Naidu is with the Department of Electrical Engineering, School of Engineering, Idaho State University, Pocatello, ID, 83201 USA e-mail: naiduds@isu.edu.

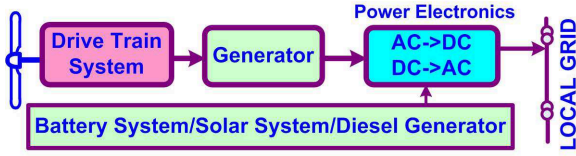


Fig. 1. Hybrid Wind Energy System

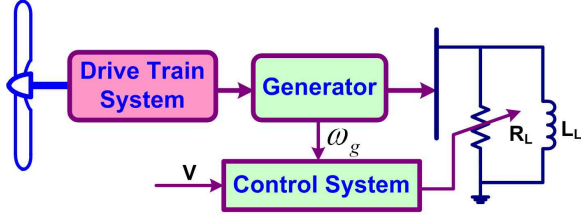


Fig. 2. Standalone WECS

where ω_r is the wind rotor rotational speed. However for the optimal power conversion purpose the torque coefficient in (1) is only dependent on the tip-speed ratio and can be approximated as the following sixth-order polynomial function of the tip-speed ratio [5]

$$C_Q(\lambda) = a_6\lambda^6 + a_5\lambda^5 + a_4\lambda^4 + a_3\lambda^3 + a_2\lambda^2 + a_1\lambda + a_0. \quad (4)$$

The power coefficient $C_P(\lambda)$ has its maximum value at the so-called optimal tip-speed ratio λ^* as illustrated in Fig. 3. Therefore, to maximize the power conversion, the WECS must operate at the optimal tip-speed ratio. However, when the wind speed changes, the tip-speed ratio is perturbed away from the optimal value as seen from (3). To maintain the optimal tip-speed ratio, the wind rotor speed ω_r must be adjusted by the control system.

The standalone PMSG model in the *direct* and *quadrature* (d, q) frame is given as [5]

$$\frac{d}{dt}i_d = -\frac{R_s + R_L}{L_d + L_L}i_d + \frac{p(L_q - L_L)}{L_d + L_L}i_q\omega_g, \quad (5)$$

$$\frac{d}{dt}i_q = -\frac{R_s + R_L}{L_q + L_L}i_q - \frac{p(L_d + L_L)}{L_q + L_L}i_d\omega_g + \frac{p\Phi_m}{L_q + L_L}\omega_g, \quad (6)$$

$$T_g = p\Phi_m i_q, \quad (7)$$

where i_d and i_q are the d - and q -components of the stator currents respectively; L_d and L_q are the d - and q -components of the stator inductances respectively; R_s is the stator resistance; R_L is the equivalent load resistance; p is the number of pole pairs; Φ_m is the linkage flux; ω_g is the high-speed or generator speed; and T_g is the generator electromagnetic torque.

The drive train system consists of a low-speed shaft connected to a high-speed shaft through a gearbox which is a rotational speed multiplier. The drive train dynamics can be represented by a rigid model as

$$J_h \frac{d\omega_g}{dt} = \frac{\eta}{i} T_r - T_g, \quad (8)$$

where J_h is the equivalent inertia transformed into the high-speed side, η and i are the gearbox efficiency and speed

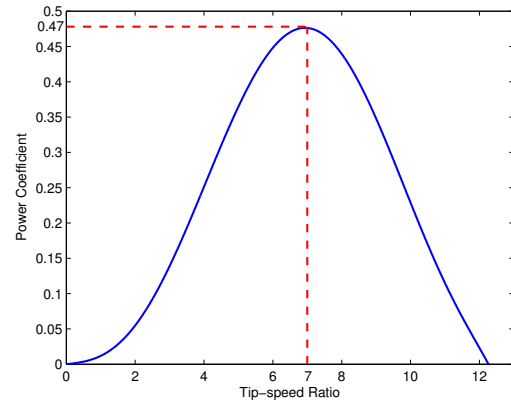


Fig. 3. Power Coefficient Curve

ratio respectively, T_r is the aerodynamic torque, and T_g is the generator electromagnetic torque.

Defining $x = [x_1 \ x_2 \ x_3]^T = [i_d \ i_q \ \omega_g]^T$ as the state variable vector, $u = R_L$ as the control input, and $y = \omega_g$ is the system output. Combining (1), (3), and (5)-(8) gives a nonlinear state space model of the standalone PMSG-based WECS:

$$\begin{bmatrix} \dot{x}_1 \\ \dot{x}_2 \\ \dot{x}_3 \end{bmatrix} = \underbrace{\begin{bmatrix} f_1(x) \\ f_2(x) \\ f_3(x) \end{bmatrix}}_{f(x)} + \underbrace{\begin{bmatrix} g_1(x) \\ g_2(x) \\ g_3(x) \end{bmatrix}}_{g(x)} u, \quad (9)$$

$$y = h(x), \quad (10)$$

where

$$f_1(x) = -\frac{R_s}{L_d + L_L}x_1 + \frac{p(L_q - L_L)}{L_d + L_L}x_2x_3, \quad (11)$$

$$f_2(x) = -\frac{R_s}{L_q + L_L}x_2 - \frac{p(L_d + L_L)}{L_q + L_L}x_1x_3 + \frac{p\Phi_m}{L_q + L_L}x_3, \quad (12)$$

$$f_3(x) = \frac{\eta\rho\pi R^3 V^2}{2iJ_h}C_Q(x_3, V) - \frac{p\Phi_m}{J_h}x_2, \quad (13)$$

and

$$g_1(x) = -\frac{1}{L_d + L_L}x_1, \quad (14)$$

$$g_2(x) = -\frac{1}{L_q + L_L}x_2, \quad (15)$$

$$g_3(x) = 0, \quad (16)$$

$$h(x) = x_3. \quad (17)$$

Note that the wind rotor speed ω_r is multiplied i times after going through the gearbox, therefore the generator speed ω_g is i times larger than the wind rotor speed. Consequently the torque coefficient $C_Q(x_3, V)$ in (13) can be expressed as

$$C_Q(x_3, V) = a_6 \left(\frac{Rx_3}{iV} \right)^6 + a_5 \left(\frac{Rx_3}{iV} \right)^5 + a_4 \left(\frac{Rx_3}{iV} \right)^4 + a_3 \left(\frac{Rx_3}{iV} \right)^3 + a_2 \left(\frac{Rx_3}{iV} \right)^2 + a_1 \left(\frac{Rx_3}{iV} \right) + a_0. \quad (18)$$

It is observed from (18) that the dynamical model (9)-(10) is highly nonlinear.

III. ADAPTIVE CONTROL METHOD

Consider a Single Input Single Output (SISO) nonlinear system defined in the region $D_x \in R^n$ as

$$\dot{x} = f(x) + g(x)u, \quad (19)$$

$$y = h(x), \quad (20)$$

where $x \in R^n$ is the state vector, $u \in R^1$ is the control input, $y \in R^1$ is the system output, $f(x) \in R^n$ and $g(x) \in R^n$ are smooth vector fields, and $h(x) \in R^1$ is a scalar smooth function. It is assumed the nonlinear system (19)-(20) has a relative degree r ($r < n$) at $x_0 \in D_x$ and internal dynamics is stable, taking derivatives of the output y with respect to time up to r times gives

$$y^{(r)} = L_f^r h(x) + \underbrace{L_g L_f^{r-1} h(x)}_{\neq 0} u, \quad (21)$$

where $L_f^r h(x)$ is the Lie derivative of $h(x)$ along the direction of the vector field $f(x)$ up to r times, $L_g L_f^{r-1} h(x)$ is the Lie derivative of $L_f^{r-1} h(x)$ along the direction of the vector field $g(x)$.

Defining $\alpha(x) = L_f^r h(x)$ and $\beta(x) = L_g L_f^{r-1} h(x)$ and rewriting (21) yields

$$y^{(r)} = \alpha(x) + \beta(x)u, \quad (22)$$

Assumption 1: The function $\beta(x)$ is positive. It means that $0 < \beta(x) < \infty$ with $\forall x \in D_x$.

Choosing the state feedback linearization control:

$$u^*(x) = \frac{1}{\beta(x)} (-\alpha(x) + v), \quad (23)$$

, then the input-output nonlinear relation (22) becomes linear as

$$y^{(r)} = v. \quad (24)$$

A. Fuzzy Approximation Strategy

The linear input-output relation (24) can be designed for stabilization or tracking with any linear methods. It is apparent that the ideal feedback linearization control (23) is only applicable if $\alpha(x)$ and $\beta(x)$ are known. However, there are uncertainties imposed on $\alpha(x)$ and $\beta(x)$ in practice, therefore the control (23) is not accurate. In this case, adaptive algorithms were proposed to realize the ideal control $u^*(x)$ by using an approximate nonlinear function $\hat{u}(x)$, called direct adaptive control, or by using approximate $\hat{\alpha}(x)$ and $\hat{\beta}(x)$ of nonlinear functions $\alpha(x)$ and $\beta(x)$, called indirect adaptive control [13], [14]. This paper presents the direct adaptive control using the fuzzy approximation.

The control problem is to drive the output y track a reference signal y_m (y_m is a smooth function). The feedback linearized control input v in (24) is defined as

$$v = y_m^{(r)} + \bar{e}_s + \gamma e_s, \quad (25)$$

where γ is a positive constant, \bar{e}_s and e_s are defined as

$$e_s = e_o^{(r-1)} + k_1 e_o^{(r-2)} + \dots + k_{r-1} e_o, \quad (26)$$

$$\bar{e}_s = \dot{e}_s - e_o^{(r)} = k_1 e_o^{(r-1)} + \dots + k_{r-1} \dot{e}_o, \quad (27)$$

$$e_o = y_m - y, \quad (28)$$

where e_s is the tracking error, e_o is the output error. Coefficients k_i are chosen such that following polynomial is Hurwitz

$$E(s) = s^{r-1} + k_1 s^{r-2} + \dots + k_{r-2} s + k_{r-1}, \quad (29)$$

The ideal control input in (23) is approximated by a fuzzy system as

$$\hat{u}(x) = \theta_u^T \xi_u(x), \quad (30)$$

where θ_u is a parameter vector including values of singleton membership function at consequent propositions of the fuzzy system rule base, $\xi_u(x)$ is a fuzzy regressive vector. θ_u is updated online such that $\hat{u}(x)$ approaches $u^*(x)$. The optimal parameter vector is

$$\theta_u^* = \arg \min_{\theta \in D_\theta} \left\{ \sup_{x \in D_x} |\theta_u^T \xi_u(x) - u^*| \right\}. \quad (31)$$

Because $u^*(x)$ is approximated by a fuzzy system possessing a finite number of rules, there exists an unavoidable structural error $\delta_u(x)$. Therefore the actual ideal control $u^*(x)$ is

$$u^*(x) = \theta_u^{*T} \xi_u(x) + \delta_u(x). \quad (32)$$

The difference between the approximate control $\hat{u}(x)$ and ideal control $u^*(x)$ is

$$\hat{u}(x) - u^*(x) = \tilde{\theta}_u^T \xi_u(x) - \delta_u(x), \quad (33)$$

where

$$\tilde{\theta}_u = \theta_u - \theta_u^* \quad (34)$$

is the approximation error.

Assumption 2: The adaptive control is chosen such that the structural error is bounded ($|\delta_u(x)| \leq \bar{\delta}_u$) with $\forall x \in D_x$ and the upper bound $\bar{\delta}_u$ is known.

Due to the presence of the structural error, an additional supervisory control u_s is added to guarantee the closed-loop stability. Therefore the real control is

$$u = \hat{u} + u_s. \quad (35)$$

B. Adaptive Law Design

The adaptive law is designed based on an *Lyapunov* analysis is presented here.

Adding and subtracting $\beta(x)u^*(x)$ into (22) gives

$$\begin{aligned} y^{(r)} &= \alpha(x) + \beta(x)u^*(x) + \beta(x)[u(x) - u^*(x)], \\ &= v + \beta(x)[u(x) - u^*(x)]. \end{aligned} \quad (36)$$

Combining (25), (28), (33), (35), and (36) gives

$$\begin{aligned} e_o^{(r)} &= y_m^{(r)} - y^{(r)}, \\ e_o^{(r)} &= y_m^{(r)} - v - \beta(x)[u(x) - u^*(x)], \\ e_o^{(r)} &= -\bar{e}_s - \gamma e_s - \beta(x)[\hat{u}(x) + u_s - u^*(x)], \\ e_o^{(r)} &= -\bar{e}_s - \gamma e_s - \beta(x)\tilde{\theta}_u^T \xi_u(x) + \beta(x)\delta_u(x) - \beta(x)u_s. \end{aligned} \quad (37)$$

Combining (27) and (37) yields the error dynamic as

$$\dot{e}_s + \gamma e_s = -\beta(x)\tilde{\theta}_u^T \xi_u(x) + \beta(x)\delta_u(x) - \beta(x)u_s. \quad (38)$$

Considering a positive semidefinite quadratic *Lyapunov* function:

$$V = \frac{1}{2\beta(x)} e_s^2 + \frac{1}{2} \tilde{\theta}_u^T Q_u \tilde{\theta}_u, \quad (39)$$

where Q_u is a positive definite weighting matrix. Taking the derivative of V with respect to time, with the observation from (34) that $\dot{\tilde{\theta}}_u = \dot{\theta}_u$, yields

$$\dot{V} = \frac{1}{\beta(x)} e_s \dot{e}_s - \frac{\dot{\beta}(x)}{2\beta^2(x)} e_s^2 + \tilde{\theta}_u^T Q_u \dot{\theta}_u. \quad (40)$$

Substituting (38) into (40) produces

$$\begin{aligned} \dot{V} &= \frac{e_s}{\beta(x)} \left[-\gamma e_s - \beta(x) \tilde{\theta}_u^T \xi_u(x) + \beta(x) \delta_u(x) \right. \\ &\quad \left. - \beta(x) u_s \right] - \frac{\dot{\beta}(x)}{2\beta^2(x)} e_s^2 + \tilde{\theta}_u^T Q_u \dot{\theta}_u, \\ \dot{V} &= -\frac{\gamma e_s^2}{\beta(x)} - e_s u_s + e_s \delta_u(x) + \tilde{\theta}_u^T (Q_u \dot{\theta}_u - \xi_u(x) e_s) \\ &\quad - \frac{\dot{\beta}(x)}{2\beta^2(x)} e_s^2. \end{aligned} \quad (41)$$

Choosing the adaptive law:

$$\dot{\theta}_u = Q_u^{-1} \xi_u(x) e_s, \quad (42)$$

and substituting (42) into (41) gives

$$\begin{aligned} \dot{V} &= -\frac{\gamma e_s^2}{\beta(x)} - e_s u_s + e_s \delta_u(x) - \frac{\dot{\beta}(x)}{2\beta^2(x)} e_s^2, \quad (43) \\ \dot{V} &\leq -\frac{\gamma e_s^2}{\beta(x)} - e_s u_s + |e_s| \left(|\delta_u(x)| \right. \\ &\quad \left. + \frac{|\dot{\beta}(x)|}{2\beta^2(x)} |e_s| \right). \end{aligned} \quad (44)$$

Assumption 3: There exist positive lower bound and upper bound of $\beta(x)$. It means $0 < \underline{\beta} \leq \beta(x) \leq \bar{\beta}$.

Assumption 4: The velocity of $\beta(x)$ is bounded. It means $|\dot{\beta}(x)| \leq \beta_v$.

Combining (44) with assumptions 3 and 4 yields

$$\dot{V} \leq -\frac{\gamma e_s^2}{\bar{\beta}} - e_s u_s + |e_s| \left(\bar{\delta}_u + \frac{\beta_v}{2\bar{\beta}^2} |e_s| \right). \quad (45)$$

Choosing the supervisory control u_s as

$$u_s = \left(\bar{\delta}_u + \frac{\beta_v}{2\bar{\beta}^2} |e_s| \right) \text{sgn}(e_s), \quad (46)$$

and substituting (46) into (45) gives

$$\dot{V} \leq -\frac{\gamma e_s^2}{\bar{\beta}} \leq 0. \quad (47)$$

Note that $e_s \text{sgn}(e_s) = |e_s|$. It is seen from (39) and (47), the positive semidefinite *Lyapunov* function V has its negative semidefinite derivative \dot{V} , therefore the closed-loop adaptive system is stable [15].

IV. ADAPTIVE CONTROL DESIGN FOR THE STANDALONE WECS

In this section the adaptive control method presented in Section III is applied to the standalone nonlinear PMSG-based WECS given in (9) and (10). The control objective is to track the optimal generator speed reference ω_g^* in order to maintain the optimal tip-speed ratio λ^* as the wind speed V changes. Unlike the feedback linearization design in [5] where authors simplified the sixth-order polynomial torque coefficient in (4) by using an approximate second-order polynomial which captures only the steady-state region,

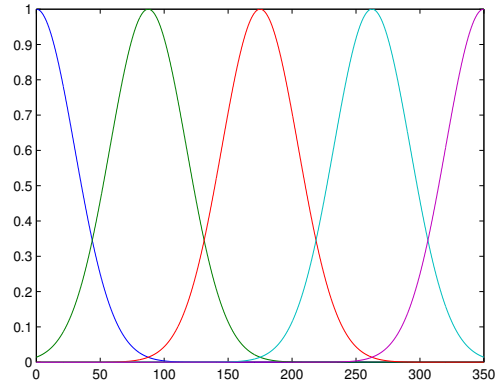


Fig. 4. Gaussian Fuzzy Sets of the Linguistic Variable x_3

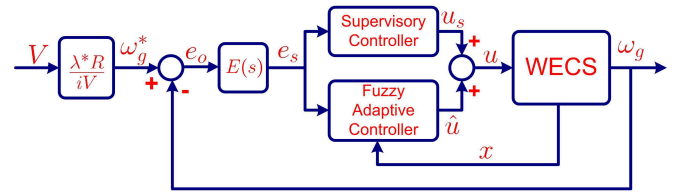


Fig. 5. Direct Fuzzy Adaptive Control Structure

our study uses the sixth-order polynomial torque coefficient which captures all operating regions.

The fuzzy model $\hat{u}(x)$ used to approximate the control $u^*(x)$ is chosen as Takagi-Sugeno model which has inference rules in the form

If x_1 is A_{1i} and x_2 is A_{2i} and x_3 is A_{3i} then $\hat{u}(x) = \theta_{ui}$, where x_1 , x_2 , and x_3 are state variables; A_{1i} , A_{2i} , and A_{3i} are fuzzy sets of linguistic variables describing x_1 , x_2 , and x_3 respectively at the i^{th} rule. The forms and number of fuzzy sets for linguistic variables are chosen based on trial and error basis. In this system fuzzy set forms were chosen as Gaussian and there are five fuzzy sets for each linguistic variable as shown in Fig. 4. Consequently there are total 125 rules.

The approximate fuzzy system in (30) is

$$\hat{u}(x) = \theta_u^T \xi_u(x),$$

where

$$\theta_u = [\theta_{u1} \ \theta_{u2} \dots \theta_{u125}]^T, \quad (48)$$

$$\xi_u(x) = [\xi_{u1}(x) \ \xi_{u2}(x) \dots \xi_{u125}(x)]^T, \quad (49)$$

$$\xi_{ui} = \frac{\mu_{A_{1i}}(x_1) \cdot \mu_{A_{2i}}(x_2) \cdot \mu_{A_{3i}}(x_3)}{\sum_{i=1}^{125} \mu_{A_{1i}}(x_1) \cdot \mu_{A_{2i}}(x_2) \cdot \mu_{A_{3i}}(x_3)}, \quad (50)$$

where ξ_{ui} is the regressor at the i^{th} rule.

The direct fuzzy adaptive control structure is shown in Fig. 5 where the adaptive controller is given in (30) with the adaptive law given in (42), and the supervisory controller is given in (46).

V. SIMULATION RESULTS

Simulations were carried out with a 3KW standalone PMSG-based WECS which has the optimal power coefficient

TABLE I
SIMULATION DATA

Wind Rotor	Drive Train	PMSG
$R = 2.5 \text{ m}$ $\rho = 1.25 \text{ kg/m}^3$	$i = 7$ $\eta = 1$ $J_h = 0.0552 \text{ kg.m}^2$	$p = 3, R_s = 3.3 \Omega$ $L_d = 0.04156 \text{ H}$ $L_q = 0.04156 \text{ H}$ $L_s = 0.08 \text{ H}$ $\Phi_m = 0.4382 \text{ Wb}$

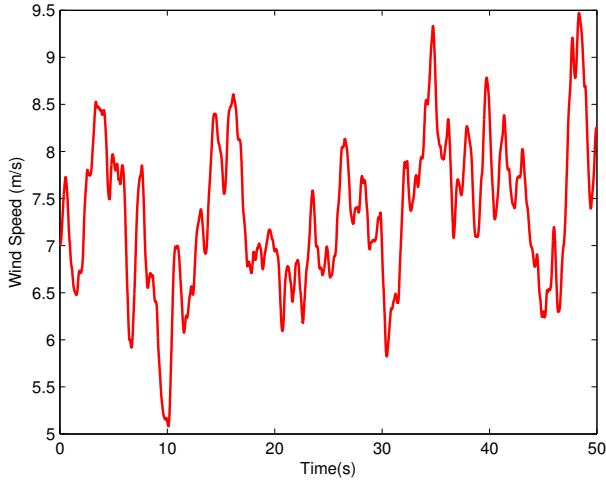


Fig. 6. Simulation Wind Speed Profile

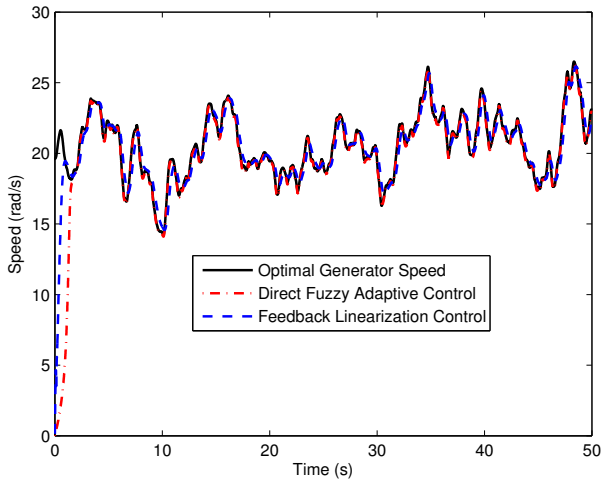


Fig. 7. Output Reference Tracking

$C_{P_{max}} = 0.478$ and the optimal tip-speed ratio $\lambda^* = 7$. Other system parameters are given Table I. Lower and upper bounds in assumption 2, 3, and 4 are $\bar{\delta}_u = 0.001$, $\beta = 1$, and $\beta_v = 30$. The nonlinear PMSG-based WECS has the relative degree $r = 2$, so parameters for the error dynamics are chosen as $\gamma = 15$ and $k_1 = 5$. The control input is set bounded as $0 < u \leq 100$. The stochastic wind profile is shown in Fig. 6. Control performances of both Direct Fuzzy Adaptive Control (DFAC) proposed in this paper and Feedback Linearization Control (FLC) proposed in [5] are compared in parallel.

Regarding the output tracking performance, Fig. 7 and 8 show both DFAC and FLC track the output reference

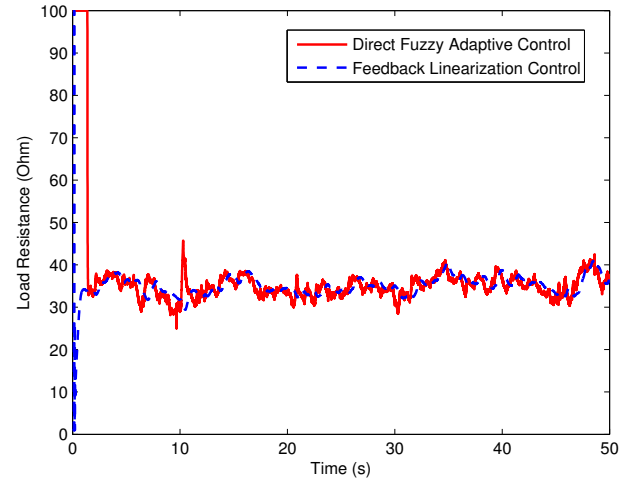


Fig. 8. Control Inputs

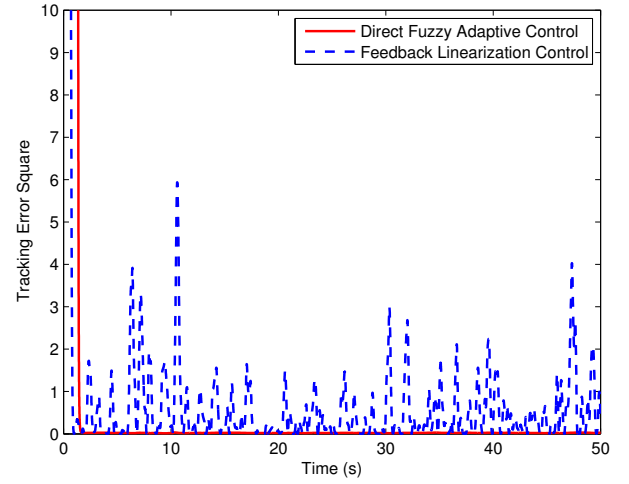


Fig. 9. Tracking Errors

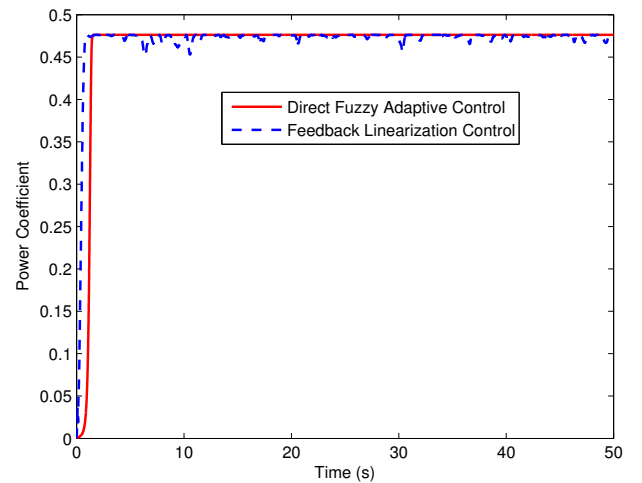


Fig. 10. Optimal Power Coefficient Maintenance

satisfactorily. However the DFAC provides better tracking than the FLC does as seen from the Fig. 9 which indicates tracking errors.

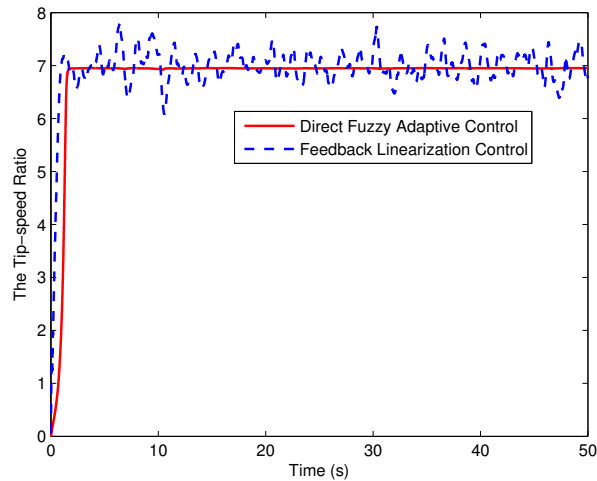


Fig. 11. Optimal Tip-speed Ratio Maintenance

Regarding the power conversion efficiency, two important factors representing the optimal power extraction are the power coefficient maintenance and tip-speed ratio maintenance under wind speed fluctuations. Fig. 10 and 11 prove the DFAC better than the FLC in optimizing the power conversion. It is obviously observed from those figures that the DFAC stays constantly steady at the optimal power coefficient and tip-speed ratio values after the transient time. Meanwhile, the FLC keeps oscillating around optimal values.

VI. DISCUSSION AND CONCLUSION

The simulation results show that the proposed DFAC is very good in dealing with the time-varying, nonlinear nature of WECS. The DFAC was also proven more effective than the FLC regarding the control performance and power capture. However, the design of DFAC requires certain assumptions to be met as stated in Section III which are not always satisfied in practice. For example, it is hard to find lower and upper bounds of the nonlinear function $\beta(x)$ and structural error $\delta_u(x)$. These values were found based on the system physical features combined with the trial and error method in this paper.

Another important note is that both DFAC and FLC require all states to be accessible. As we know that system states are not available sometime and/or somewhere; consequently the DFAC and FLC are not applicable in those situations. Therefore, an extension of this study would be constructing a nonlinear observer to estimate unavailable states and integrating the nonlinear observer into the DFAC scheme.

REFERENCES

- [1] M. Stiebler, *Wind Energy Systems for Electric Power Generation*. Springer-Verlag, 2008.
- [2] C. Abbey, K. Strunz, and G. Joos, "A knowledge-based approach for control of two-level energy storage for wind energy systems," *Energy Conversion, IEEE Transactions on*, vol. 24, no. 2, pp. 539–547, June 2009.
- [3] S. Teleke, M. Baran, A. Huang, S. Bhattacharya, and L. Anderson, "Control strategies for battery energy storage for wind farm dispatching," *Energy Conversion, IEEE Transactions on*, vol. 24, no. 3, pp. 725–732, Sept. 2009.
- [4] S. Teleke, M. Baran, S. Bhattacharya, and A. Huang, "Optimal control of battery energy storage for wind farm dispatching," *Energy Conversion, IEEE Transactions on*, vol. 25, no. 3, pp. 787–794, Sept. 2010.

- [5] I. Munteanu, A. Bratcu, N. Cutululis, and E. Ceanga, *Optimal Control of Wind Energy Systems: Toward a Global Approach*. Springer, 2008.
- [6] K. Astrom and T. Hagglund, *Adaptive Control*. Dover Publications Inc., Mineola, N.Y., U.S., 2008, second Edition.
- [7] W. Dinghui, X. Lili, and J. Zhicheng, "Fuzzy adaptive control for wind energy conversion system based on model reference," in *Control and Decision Conference, 2009. CCDC '09. Chinese*, Jun. 2009, pp. 1783–1787.
- [8] J. Qi and Y. Liu, "PID control in adjustable-pitch wind turbine system based on fuzzy control," in *Industrial Mechatronics and Automation (ICIMA), 2010 2nd International Conference on*, vol. 2, May 2010, pp. 341–344.
- [9] X. Yao, H. Wen, Y. Deng, and Z. Zhang, "Research on rotor excitation neural network PID control of variable speed constant frequency wind turbine," in *Electrical Machines and Systems, 2007. ICEMS. International Conference on*, Oct. 2007, pp. 560–565.
- [10] X. Yao, X. Su, and L. Tian, "Wind turbine control strategy at lower wind velocity based on neural network PID control," in *Intelligent Systems and Applications, 2009. ISA 2009. International Workshop on*, May 2009, pp. 1–5.
- [11] —, "Pitch angle control of variable pitch wind turbines based on neural network PID," in *Industrial Electronics and Applications, 2009. ICIEA 2009. 4th IEEE Conference on*, May 2009, pp. 3235–3239.
- [12] Z. Xing, Q. Li, X. Su, and H. Guo, "Application of BP neural network for wind turbines," in *Intelligent Computation Technology and Automation, 2009. ICICTA '09. Second International Conference on*, vol. 1, Oct. 2009, pp. 42–44.
- [13] L.-X. Wang, *A Course in Fuzzy Systems and Control*. Prentice-Hall, Inc., Upper Saddle River, New Jersey, U.S., 1996.
- [14] H. T. Huynh, *Intelligent Control Systems*. Ho Chi Minh National University Press, 2006.
- [15] H. Khalil, *Nonlinear Systems, 2nd Edition*. Prentice-Hall, Inc., Upper Saddle River, New Jersey, U.S., 1996.